

Validation of a Real-Time Geometry-Based Stochastic Channel Model for Vehicular Scenarios

Markus Hofer*, Zhinan Xu*, Dimitrios Vlastaras[†], Bernhard Schrenk*,
David Löschenbrand*, Fredrik Tufvesson[†] and Thomas Zemen*

*AIT Austrian Institute of Technology, Vienna, Austria

[†]Department of Electrical and Information Technology, Lund University, Sweden

Email: markus.hofer@ait.ac.at

Abstract—The performance of wireless communication systems is fundamentally determined by wireless communication channel properties. Wireless vehicular communication channels exhibit multipath propagation and non-stationary channel statistics. Methods and tools for the repeatable test of wireless communication systems and signal processing algorithms in such environments are urgently needed to enable the development of reliable communication links with low-latency. In this paper we present the measurement and validation of a real time channel emulation method for non-stationary vehicular scenarios based on a geometry-based stochastic channel model.

Index Terms—real-time, channel emulation, SDR, geometry-based stochastic channel model, FPGA, software defined radio

I. INTRODUCTION

Non-stationary propagation conditions are key aspects of wireless communication channels that connect vehicles. For vehicular scenarios empiric measurement data [1–4] exists, and channel modelling techniques based on geometry-based stochastic channel models (GSCMs) [5–7] are well established and validated. GSCMs represent the propagation scenarios by a sum of propagation paths that are defined by point scatterers placed according to a spatial distribution. Different scatterer types are defined such as discrete stationary scatterer (parked vehicles, road signs), mobile scatterers (moving vehicles) and diffuse scatterers (e.g. trees). Real-time channel emulation for non-stationary scenarios based on a GSCM is a missing component that we validate for the first time in this paper.

Commercially available channel emulation solutions from Spirent [8] and Anite [9] as well as software defined radio (SDR) based channel emulator solutions [10–16] are all based on tap delay line (TDL) models. Due to the underlying TDL model, all these emulators share the main drawback that path delays can be only set in integer multiples of the sampling rate.

A new low-complexity reduced-rank subspace model was introduced by Kaltenberger et al. [17–19] to emulate a GSCM with real-valued path delay and Doppler shift. In [20] we presented a first digital fixed-point field programmable gate array (FPGA) implementation of this concept. The GSCM computation and the subspace projection is performed on a general purpose multi-core personal computer (PC). The

subspace coefficients represent a highly compressed channel representation that is streamed to the SDR to compute the convolution with the input signal using an efficient fixed point FPGA implementation [21]. With this approach the computational complexity on the FPGA is *independent* of the number of multipath components.

The scientific contribution of this paper is the validation of the implementation of the GSCM by channel sounding measurements with the RUSK Lund channel sounder and comparing the measurements with a Matlab co-simulation.

II. SYSTEM MODEL

To emulate the effects of wireless wave propagation a real-time emulator convolves the input signal with the time-variant channel impulse response. The architecture of our emulator is shown in Fig. 1 (see also [20]).

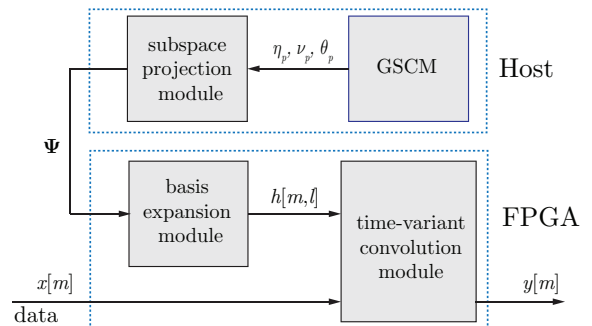


Fig. 1: Channel emulator architecture [20]

To realistically model the non-stationary properties of wireless channel propagation we assume that the channel propagation parameters originate from a GSCM [5]. We describe the non-stationary time-variant frequency response [20, 22–25],

$$g_{\text{ph}}(t, f) = \sum_{p=0}^{P-1} \eta'_p(t) e^{-j2\pi\tau_p(t)f}, \quad (1)$$

as the superposition of P individual propagation paths with time-variant path delay $\tau_p(t)$. Each path is characterized by the complex time-variant weighting coefficient $\eta'_p(t) =$

$a_p(t)e^{j2\pi\phi_p}$ with amplitude $a_p(t)$ and initial phase ϕ_p . The channel can be approximated as wide-sense stationary within the stationary time T_{stat} [1, 2]. We assume that within a stationarity region the amplitude of a path does not change, i.e., $\eta'_p(t) \approx \eta'_p$ for $t_1 \leq t < t_1 + T_{\text{stat}}$ and that the velocity between transmitter and receiver stays constant. Thus, we model the time-variant path delay with a linear model [20, 22]

$$\tau_p(t) = \tau_p(0) - \frac{f_p}{f_c}t. \quad (2)$$

The initial path delay $\tau_p(0)$ is determined by the distance between transmitter and receiver, f_c denotes the carrier frequency of the system and f_p denotes the Doppler shift of path p . The Doppler shift is defined by

$$f_p = f_c \frac{v_p}{c_0}, \quad (3)$$

with v_p denoting the relative velocity between transmitter and receiver that is determined by the geometry of the scenario (see e.g. [5, 23] for more information) and c_0 the speed of light. With (2) and assuming that the system bandwidth is much smaller than the carrier frequency f_c , which is true for most communication systems [25, Ch. 1], we obtain the time-variant channel transfer function as

$$g_{\text{Ph}}(t, f) = \sum_{p=0}^{P-1} \eta_p e^{j2\pi f_p t} e^{-j2\pi\tau_p(0)f'}, \quad (4)$$

where we define $\eta_p = \eta'_p e^{-j2\pi\tau_p(0)f_c}$.

Sampled Channel Transfer Function

We emulate the channel for a finite system bandwidth B . To allow for realistic input/output filters of an implemented system we oversample $g_{\text{Ph}}(t, f)$ by a factor f_{OSF} , i.e., $B' = f_{\text{OSF}}B$. We sample with $T_C = 1/B'$. Considering a band-limiting filter $g_R(f)$ and using (2) we obtain

$$\begin{aligned} g[m, q] &:= g_R(qF_s)g_{\text{Ph}}(mT_C, qF_s) \\ &= g_R[q] \sum_{p=0}^{P-1} \eta_p e^{-j2\pi q\theta_p} e^{j2\pi m\nu_p} \end{aligned} \quad (5)$$

where $\nu_p = f_p T_C$ denotes normalized Doppler shift and $\theta_p = \tau_p(0)/(NT_C)$ normalized path delay with $|\nu_p| < \frac{1}{2}$ and $0 \leq \theta_p < 1$.

To emulate the effects of a wireless propagation channel the emulator convolves the input signal $x[m]$ with the time-variant channel impulse response (CIR) $h[m, l]$ to obtain the output signal

$$y[m] = \sum_{l=0}^{L-1} h[m-l, l]x[m-l], \quad (6)$$

with l denoting the index in the delay domain and L the number of delay taps. We obtain $h[m, l]$ by the inverse discrete Fourier transform (IDFT) of the time-variant transfer function $g[m, q]$.

To reduce the streaming bandwidth between SDR and PC we compress the CIR using a reduced-rank basis-expansion

model (BEM) as explained in [17, 20]. A subspace-projection module utilizes the path weight η_p , normalized Doppler shift ν_p and normalized path delay θ_p of each propagation path to obtain the basis coefficient matrix Ψ that describes the evolution of the channel. The accuracy of the description depends on the number of utilized basis coefficients as shown in [20]. On the FPGA the CIR is reconstructed using the basis coefficient matrix Ψ and basis vectors, see Fig. 1. We utilize discrete prolate spheroidal sequences [26] for the compression and reconstruction of the CIR. The basis coefficients are periodically updated in *real-time* with T_{stat} .

III. MEASUREMENT AND VALIDATION OF THE CHANNEL EMULATOR

For the validation of our real-time GSCM implementation we use a road intersection crossing scenario. In [6] a GSCM model for this particular road intersection scenario was developed. We validate the functionality of the channel emulator by comparison with a numerical co-simulation that is explained in [20]. In the following we introduce the emulation parameters, show the measurement setup and describe the evaluation method in more detail.

A. Emulation Parameters

We set the carrier frequency of the system to $f_c = 5.7$ GHz. We implement the emulator for a bandwidth of 10 MHz, a maximum path delay of $\tau_{\text{max}} = 1.6 \mu\text{s}$ and a maximum speed of $v_{\text{max}} = 400$ km/h. The oversampling factor is set to $f_{\text{OSF}} = 2$ which leads to $T_C = 50$ ns. We choose the stationarity region length to $T_{\text{stat}} = 256 \mu\text{s}$ ($M = 5120$) which is equal to an update rate of the subspace coefficients $1/T_{\text{stat}} \approx 3.907$ kHz. The number of sample points in the frequency direction is set to $N = 128$.

As SDR we use a National Instruments (NI) USRP-2954R [27] that is equipped with an Xilinx Kintex-7 FPGA. The measured overall system delay is $\tau_{\text{proc}} \approx 5.3 \mu\text{s}$.

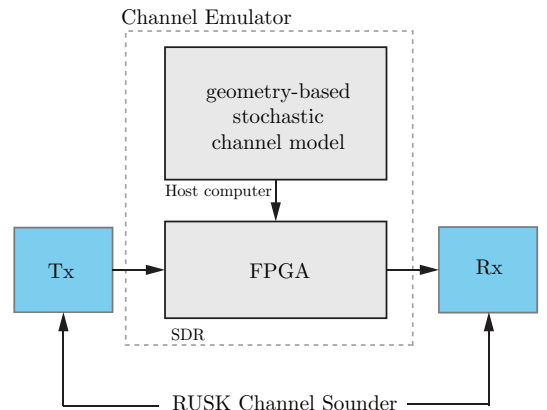


Fig. 2: Measurement Setup

B. Measurement Setup

The measurement setup is shown in Fig. 2. The RUSK channel sounder measures the discrete frequency response $g[u, q] = g(t_s u, f_s q)$ of the channel emulator by periodically sampling $g(t, f)$ in time and frequency direction [1, 2]. Here, $u \in \{0, \dots, U - 1\}$ represents the discrete time index sampled at t_s with U being the total number of snapshots and $q \in \{0, \dots, Q - 1\}$ denotes the discrete frequency index with Q the number of frequency bins. The frequency resolution is defined by $f_s = B_M/Q$.

The length of the sounding sequence was set to $T = 12.8 \mu\text{s}$ which corresponds to the maximum measurable excess delay, i.e., $\tau_{\text{Mmax}} = T$. We recorded the CIR with a repetition rate of $t_s = 102.4 \mu\text{s}$ which results in a maximum resolvable Doppler shift of

$$\nu_D = \frac{1}{2t_s} = 4.883 \text{ kHz}. \quad (7)$$

For the measurement we record $S_t = 100000$ snapshots which is equal to a measurement time of $T_{\text{meas}} = 10.24 \text{ s}$. We set the measurement bandwidth to $B_M = 100 \text{ MHz}$. The bandwidth was separated in $Q = 1281$ frequency bins which results to $f_s = B_M/Q = 78.06 \text{ kHz}$. To minimize the local oscillator (LO) leakage due to I/Q impairments in the direct down/up conversion in the radio frequency front ends of the USRP, we utilize a digital I/Q impairment correction. Furthermore, we use single side band emulation with a digital intermediate frequency to shift the LO leakage out of the emulated channel.

C. Measurement Evaluation

The performance of the channel emulator is characterized by the local scattering function (LSF) $\hat{C}[k_t; n, p]$ explained in [1, 28–33]. We denote $n \in \{0, \dots, M_f - 1\}$ as the delay index and $p \in \{-M_t/2, \dots, M_t/2 - 1\}$ as Doppler index, respectively. The time index of each stationarity region is $k_t \in \{0, \dots, \lfloor S_t/M_t - 1 \rfloor\}$ and correspond to the center of the stationarity regions. For the LSF evaluation we set $M_t = 400$ and $M_f = 128$ which corresponds to a stationarity region of $T_{\text{LSF}} = 41 \text{ ms}$ in time and $B = B_{\text{LSF}} \approx 10 \text{ MHz}$ in frequency.

The power delay profile (PDP) and Doppler spectral density (DSD) are calculated as a summation of the LSF over the Doppler or delay domain, respectively [1, 2], i.e.,

$$\hat{\mathcal{P}}_\tau[k_t; n] = \frac{1}{M_t} \sum_{p=-M_t/2}^{M_t/2-1} \hat{C}[k_t; n, p] \quad (8)$$

and

$$\hat{\mathcal{P}}_\nu[k_t; n] = \frac{1}{M_f} \sum_{p=0}^{M_f-1} \hat{C}[k_t; n, p]. \quad (9)$$

As validation we show a comparison of the time-variant PDP and the time-variant DSD obtained by means of the LSF [1]. The results are normalized to the maximum received power of the LSF. In Fig. 3 we show the PDP of (a) the numerical GSCM evaluation and (b) the measurement data of the channel emulator. In Fig. 4 we show the same comparison for the DSD.

We compare Fig. 3 and Fig. 4 via visual inspection and

obtain an excellent match between numerical co-simulation and channel emulation. The emulator is capable of emulating the non-stationary channel properties of the road-intersection crossing scenario. The difference in the noise floors originates from not considering thermal noise for the numerical co-simulation.

IV. CONCLUSION

In this paper we present the validation measurement of a real-time channel emulator. The emulator uses a separation in two components, the first one being the GSCM calculated on a general purpose multicore PC in *real-time* and the second one being the convolution implemented on a SDR. The emulator uses a reduced-rank channel model to compress the CIR that is transmitted to the SDR where it is convolved with the input signal. A measurement with the RUSK Lund channel sounder showed an excellent match of the emulated channels with a numerical co-simulation via visual inspection. The real-time emulation method allows repeatable testing of vehicular communication scenarios. The high flexibility of our channel emulator, i.e., the possibility to adapt the GSCM to other scenarios like highway, merging lanes, etc., makes it a key component for testing wireless communication systems and closely linked control algorithms for connected autonomous vehicles.

ACKNOWLEDGEMENT

This work has been conducted within the ENABLE-S3 project that has received funding from the ECSEL Joint Undertaking under grant agreement No 692455. This Joint Undertaking receives support from the European Union's Horizon 2020 research and innovation programme and Austria, Denmark, Germany, Finland, Czech Republic, Italy, Spain, Portugal, Poland, Ireland, Belgium, France, Netherlands, United Kingdom, Slovakia, Norway. ENABLE-S3 is funded by the Austrian Federal Ministry of Transport, Innovation and Technology (BMVIT) under the program "ICT of the Future" between May 2016 and April 2019. Furthermore, this work was partially funded by the Austrian research funding association (FFG) under the scope of an industrial PhD and by a short term scientific mission of the COST action 1504 (IRACON). The authors would also like to thank Olivier Renaudin for valuable discussions and Carl Gustafson and Jose Flordelis for their collaboration during the measurements.

REFERENCES

- [1] L. Bernadó, T. Zemen, F. Tufvesson, A. F. Molisch, and C. F. Mecklenbrauker, "Delay and Doppler spreads of nonstationary vehicular channels for safety-relevant scenarios," *IEEE Transactions on Vehicular Technology*, vol. 63, no. 1, pp. 82–93, Jan. 2014.
- [2] L. Bernadó, T. Zemen, F. Tufvesson, A. F. Molisch, and C. F. Mecklenbrauker, "Time- and frequency-varying K -factor of non-stationary vehicular channels for safety-relevant scenarios," *IEEE Transactions on Intelligent Transportation Systems*, vol. 16, no. 2, pp. 1007–1017, April 2015.
- [3] A. Paier, L. Bernadó, J. Karedal, O. Klemp, and A. Kwoczek, "Overview of vehicle-to-vehicle radio channel measurements for collision avoidance applications," in *IEEE 71st Vehicular Technology Conference (VTC)*, Taipei, Taiwan, May 2010.

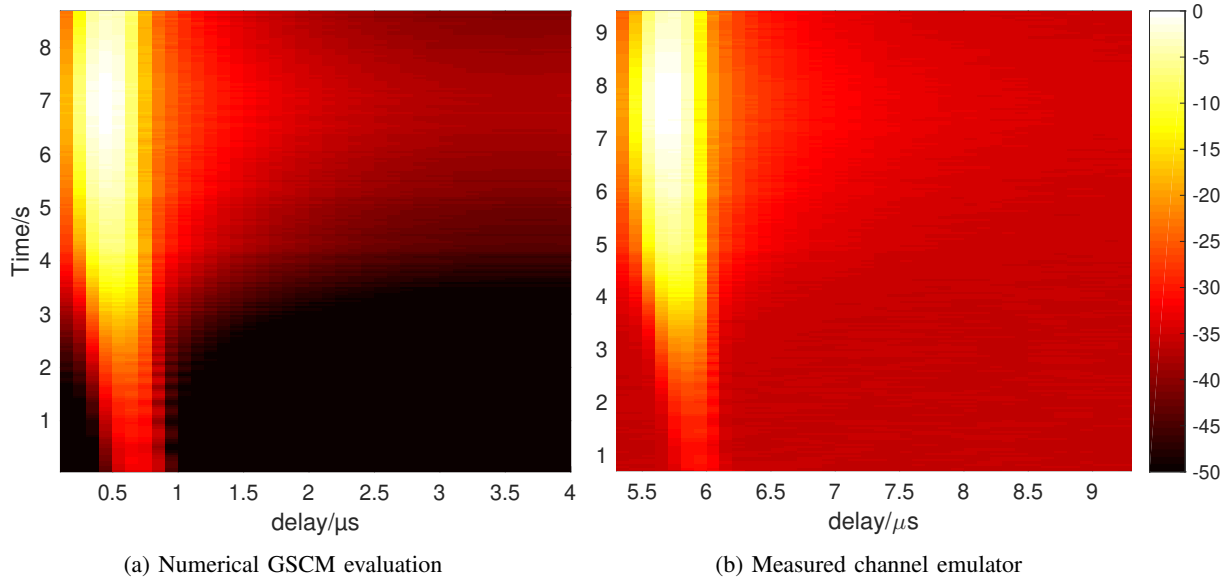


Fig. 3: Comparison of the PDP for the road intersection.

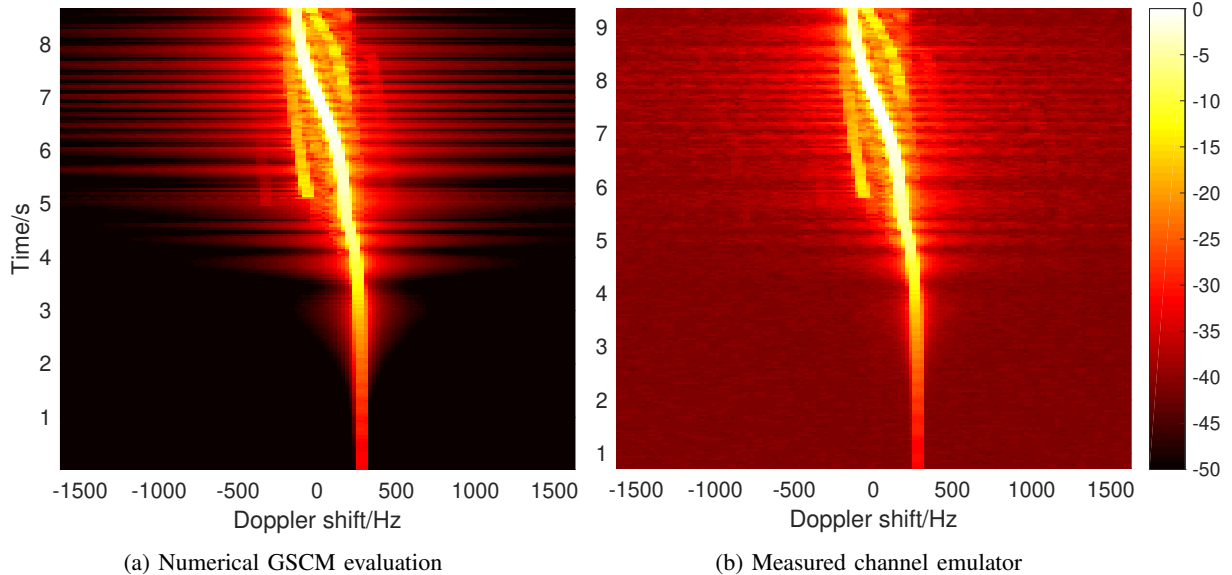


Fig. 4: Comparison of the DSD for the road intersection.

- [4] O. Renaudin, V.-M. Kolmonen, P. Vainikainen, and C. Oestges, "Wide-band MIMO car-to-car radio channel measurements at 5.3 GHz," in *2008 IEEE 68th Vehicular Technology Conference (VTC Fall)*, 2008.
- [5] J. Karedal, F. Tufvesson, N. Czink, A. Paier, C. Dumard, T. Zemen, C. F. Mecklenbräuker, and A. F. Molisch, "A geometry-based stochastic mimo model for vehicle-to-vehicle communications," *IEEE Transactions on Wireless Communications*, vol. 8, no. 7, pp. 3646–3657, Jul. 2009.
- [6] Z. Xu, L. Bernadó, M. Gan, M. Hofer, T. Abbas, V. Shivaldova, K. Mahler, D. Smely, and T. Zemen, "Relaying for IEEE 802.11p at road intersection using a vehicular non-stationary channel model," in *6th International Symposium on Wireless Vehicular Communications (WIVEC 2014)*, Vancouver, Canada, September 2014.
- [7] K. Mahler, W. Keusgen, F. Tufvesson, T. Zemen, and G. Caire, "Measurement-based wideband analysis of dynamic multipath propagation in vehicular communication scenarios," *IEEE Transactions on Vehicular Technology*, vol. 66, no. 6, pp. 4657–4667, June 2017.
- [8] Accessed: 2017-01-15. [Online]. Available: <http://www.spirent.com/>
- [9] Accessed: 2017-01-15. [Online]. Available: <http://www.anite.com/>
- [10] (2013, May) Real-time MIMO channel emulation on the NI PXIe-5644R. National Instruments. Accessed: 2016-01-15. [Online]. Available: <http://http://www.ni.com/example/31556/en/>
- [11] D. Vlastaras, S. Malkowsky, and F. Tufvesson, "Stress test of vehicular communication transceivers using software defined radio," in *2015 IEEE 81st Vehicular Technology Conference (VTC Spring)*, vol. 41, no. 2, May 2015, pp. 1–4.
- [12] G. Ghiaasi, M. Ashury, D. Vlastaras, M. Hofer, Z. Xu, and T. Zemen, "Real-time vehicular channel emulator for future conformance tests of wireless ITS modems," in *IEEE 10th European Conference on Antennas and Propagation (EuCAP)*, April 2016.
- [13] "MKG Sys," Accessed: 2016-01-15. [Online]. Available: <https://www.mkgsys.com/>
- [14] T. Fernández-Caramés, M. González-López, and L. Castedo, "FPGA-based vehicular channel emulator for real-time performance evaluation of IEEE 802.11p transceivers," *EURASIP Journal on Wireless Communications and Networking*, vol. 2010, no. 1, p. 607467, 2010.
- [15] J. Matai, P. Meng, L. Wu, B. Weals, and R. Kastner, "Designing a

- hardware in the loop wireless digital channel emulator for software defined radio," in *2012 International Conference on Field-Programmable Technology*, Dec. 2012, pp. 206–214.
- [16] T. Blazek, C. Mecklenbraüker, G. Ghiaasi, D. Smely, and M. M. Ashury, "Vehicular channel models: A system level performance analysis of tapped delay line models," in *IEEE Proceedings of the 15th International Conference on ITS Telecommunications*, 2017, Warsaw, Poland; 2017-05-29 – 2017-05-31.
- [17] F. Kaltenberger, T. Zemen, and C. W. Ueberhuber, "Low-complexity geometry-based MIMO channel simulation," *Eurasip Journal on Advances in Signal Processing*, vol. 2007, no. 1, p. 095281, 2007.
- [18] F. Kaltenberger, "Low complexity simulation of wireless channels using discrete prolate spheroidal sequences," Ph.D. dissertation, Technical University Vienna, May 2007.
- [19] F. Kaltenberger, G. Steinböck, G. Humer, and T. Zemen, "Low-complexity geometry based MIMO channel emulation," *European Space Agency. (Special Publication) ESA SP*, vol. 626 SP, no. October, 2006.
- [20] M. Hofer, Z. Xu, and T. Zemen, "Real-time channel emulation of a geometry-based stochastic channel model on a SDR platform," in *IEEE 18th International Workshop on Signal Processing Advances in Wireless Communications (SPAWC)*, Sapporo, Japan, July 2017.
- [21] M. Hofer and T. Zemen, "Verfahren zur Emulation eines Funkkanals," *Austrian Patent application A51024/2016*, filed 2016.
- [22] T. Zemen, L. Bernadó, N. Czink, and A. Molisch, "Iterative time-variant channel estimation for 802.11p using generalized discrete prolate spheroidal sequences," *IEEE Transactions on Vehicular Technology*, vol. 61, no. 3, pp. 1222–1233, March 2012.
- [23] N. Czink, F. Kaltenberger, Y. Zhou, L. Bernadó, T. Zemen, and X. Yin, "Low-complexity geometry-based modeling of diffuse scattering," *Proceedings of the Fourth European Conference on Antennas and Propagation (EuCAP)*, no. i, pp. 1–4, 2010.
- [24] D. Tse and P. Viswanath, *Fundamentals of Wireless Communication*. New York, NY, USA: Cambridge University Press, 2005.
- [25] F. Hlawatsch and G. Matz, *Wireless Communications Over Rapidly Time-Varying Channels*, 1st ed. Academic Press, 2011.
- [26] D. Slepian, "Prolate spheroidal wave functions, fourier analysis, and uncertainty-V: The discrete case," *Bell System Technical Journal*, vol. 57, no. 5, pp. 1371–1430, May 1978.
- [27] *Device Specifications, NI USRP-2594R, 10 MHz to 6 GHz Tunable RF Transceiver*, National Instruments.
- [28] G. Matz, "On non-WSSUS wireless fading channels," *IEEE Transactions on Wireless Communications*, vol. 4, no. 5, pp. 2465–2478, Sept 2005.
- [29] —, "Doubly underspread non-WSSUS channels: analysis and estimation of channel statistics," in *2003 4th IEEE Workshop on Signal Processing Advances in Wireless Communications - SPAWC 2003 (IEEE Cat. No.03EX689)*, June 2003, pp. 190–194.
- [30] D. J. Thomson, "Spectrum estimation and harmonic analysis," *Proceedings of the IEEE*, vol. 70, no. 9, pp. 1055–1096, 1982. [Online]. Available: http://ieeexplore.ieee.org/xpls/abs_all.jsp?arnumber=1456701
- [31] L. Bernadó, T. Zemen, A. Paier, J. Karedal, and B. H. Fleury, "Parametrization of the local scattering function estimator for vehicular-to-vehicular channels," in *2009 IEEE 70th Vehicular Technology Conference Fall*, Sept 2009, pp. 1–5.
- [32] L. Bernadó, T. Zemen, F. Tufvesson, A. F. Molisch, and C. F. Mecklenbraeuer, "The (in-) validity of the WSSUS assumption in vehicular radio channels," in *2012 IEEE 23rd International Symposium on Personal, Indoor and Mobile Radio Communications - (PIMRC)*, Sept 2012, pp. 1757–1762.
- [33] E. Zöchmann, C. Mecklenbraeuer, M. Lerch, S. Pratschner, M. Hofer, D. Loeschbrand, J. Blumenstein, S. Sangodoyin, G. Artner, S. Caban, T. Zemen, A. Prokes, M. Rupp, and A. F. Molisch, "Measured delay and Doppler profiles of overtaking vehicles at 60 GHz," in *12th European Conference on Antennas and Propagation (EUCAP) - submitted*, April 2018.